Shock Tube Studies of the Rate Constant for Chemical Excitation of Hydroxyl Radicals

Tohru KOIKE and Kihei MORINAGA

Department of Chemistry, National Defense Academy, Hashirimizu, Yokosuka 239

(Received August 7, 1975)

The $OH(^2\Sigma^{+2}\text{-}\Pi)$ chemiluminescence in the partial equilibrium region of the H_2—O_2 reaction in mixtures with $H_2/O_2/Ar=2/2/96$, $P_1=5$, 10, 20 Torr was studied in 1250—2000 K incident shock waves. The comparison between the temperature dependence of the $OH(^2\Sigma^+)$ emission and that of the computer simulation of the H_2—O_2 reaction yields the activation energy of the chemical excitation process, assuming the same bi-radical process as former investigators used. The evaluated $OH(^2\Sigma^+)$ profile, based on a simulation in which the chemical excitation, radiative, and non-radiative processes are accounted for, depends on the pre-exponential factor of the chemical excitation process. The correlations between the temperature dependence of the evaluated $OH(^2\Sigma^+)$ profile and that of the emission profile in the partial equilibrium region gave the pre-exponential factor of the chemical excitation process. Thus, we could estimate the rate constant for $O+H+Ar=OH(^2\Sigma^+)+Ar$ to be $1.0\times10^9\times\exp(-11000\text{ cal}/RT)$.

The reactions of hydrogen and/or hydrocarbons with oxygen are accompanied by the emission of $OH(^2\Sigma^+-{}^2\Pi)$ transitions. The origin of $OH(^2\Sigma^+)$, hereafter OH*, could be attributed to both thermal and chemical excitations.

Kinetic studies of the OH* emission have been performed in $H_2/O_2/N_2$ flame,[1] in shock heated H_2/air mixtures,[2] H_2/O_2/Ar mixtures,[3] H_2/O_2/CO/Ar mixtures,[4] and in a flow system of O and H associations.[5]

Gardiner *et al.*[3] made a detailed comparison between the growth constant of the OH* emission and that of the ground state OH concentration measured by the Bi-lamp absorption technique; they concluded that the chemical excitation process or pre-association process of OH* is $O+H+M=OH^*+M$. Schott *et al.*[4] reached the same conclusion through the comparison between the OH* growth constant and the O growth constant, which were observed *via* OH* emission and CO+O emission using their end-on technique in shock tube experiments.

Strong evidence for the above conclusion was given by Schiff *et al.*,[5] who made it clear that the intensity of the OH* emission which accompanies O+H association in a microwave discharge flow system is proportional to the concentration product of ground state O and H.

Further studies of the OH chemiluminescence in a shock heated hydrogen/oxygen reaction were performed in the present work to evaluate the rate constant of the chemical excitation process of hydroxyl radicals in gas phase, accepting the above mechanism and adpoting a computer simulation technique for the estimation of the over-all reaction scheme.

Experimental

Shock Tube. Incident shock waves were actuated in the shock tube shown in Fig. 1, where the driver section A is made of a mild steel pipe of inner diameter 8.9 cm and length 120 cm, and the test section B is an extruded rectangular brass tubing of inner cross section 3.2×7.2 cm, thickness 0.4 cm, and length 400 cm, with three quartz windows of 10 mm thickness located 300 cm downstream from the diaphragm section. The windows and a triggering thermal gauge whose location is 5 cm upstream from the windows were carefully flat mounted at the bottoms onto the test section, avoiding any aerodynamic disturbance in the tube. The triggering gauge is a vacuum deposited thin tin film and the other five thermal gauges positioned downstream from the windows at 10 cm intervals are of thin platinum deposited by the baking of brush-painted Hanovia solution. The diaphragm section D was devised to employ the two diaphragm method but natural bursts of a single diaphragm were adopted throughout the present experiments. The diaphragms were press scored aluminium plates of 0.2 mm thickness. The test section could be evacuated to less than 1 micron by an oil diffusion pump with a liquid nitrogen trap and showed a leak rate of less than 2 micron/30 min.

Optical System and Electronic Devices. The emission from the reacting gas was monitored by a S-13 response photomultiplier (Hamamatsu-TV R292) with a filter which consisted of 3 mm of Corning 9863 glass and 6 mm of 50 g/100 g solution of $NiSO_4\cdot6H_2O$. This filter combination

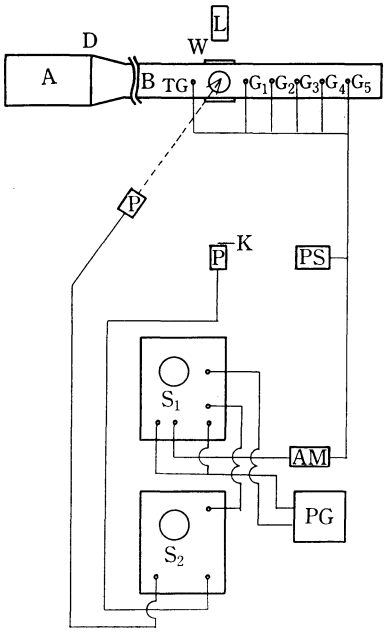

Fig. 1. Block Diagram of Apparatus.
A: Driver section, B: Test section, D: Diaphragm section, TG: Trigger gauge, G_1—G_5: Thermal gauges, W: Observation windows, L: Laser, K: Knife-edge, P: Photomultipliers, PS: Power supply, AM: Amplifier, PG: Pulse generator (Time mark, Triangle wave), $S_1\cdot S_2$: Oscilloscopes.

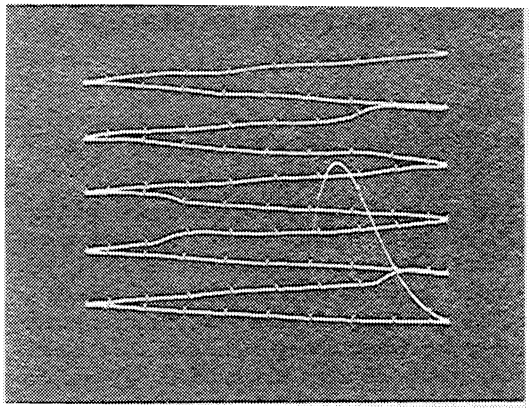

Fig. 2a. Signals of trigger gauge TG and thermal gauges G_1—G_5 are displayed on Raster sweep with 5-μs time marks.
$U_1 = 1350$ m/s, $T_2 = 1840$ K.

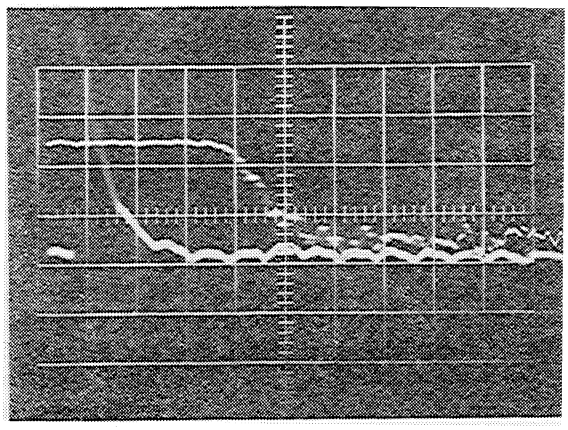

Fig. 2b. Profiles of OH* emission and laser schlieren.
Upper trace: OH* emission, gain = 1 mV/div.
Lower trace: Laser schlieren, gain = 10 mV/div.
Sweep rate = 10 μs/div.

had about 50% transmission at 306.7 nm, and its high- and low-cutoffs were 360.0 nm and 240.0 nm, respectively. Between the photomultiplier and the shock tube window two 2 mm slits were installed at a 20 cm separation. The emission from the reacting gas was observed through the slits in the direction in accordance with the minor latus of the rectangular cross section of the shock tube. A laser schlieren technique was adopted to detect any abnormality of the shock waves and any data with an abnormal laser schlieren image was discarded. The signals from the thermal resistance gauges were displayed on a Raster sweep oscilloscope along with 5 micro-second time marks from a quartz oscillator. An oscillogram of the Raster sweep is shown in Fig. 2a.

Gas Mixtures. The gases were taken from commercial cylinders whose purities, as assayed by the manufacturer, were not less than 99.9%, and were used without further purifications. Gas mixtures of the desired compositions were prepared manometrically and left to stand for at least 24 h before use. Blank tests of the emission were performed in the same manner as in the actual runs with Ar gas and H_2/Ar gas, and no appreciable emission was observed in either case.

The Computer Program. The computer program used in the present work was provided through the courtesy of W. C. Gardiner, Jr.,* and C. B. Wakefield and was modified to match the NEAC 2200 system. It was devised to calculate any of the incident or reflected shock waves with ideal, laminar, or turbulent flows. The thermodynamic data from the JANAF thermochemical tables[6] are included in it in the form of virial equations. Given the reaction mechanism to be a group of elementary reactions with forward rate constants, the program integrates the assembly of first order linear differential equations of the forward and reverse reactions *via* an implicit Adams method or Gear method, and gives the concentration profile of any desired species in relation to the time elapsed after the shock arrivals.

Results and Discussion

In studying the chemical excitation of OH*, Gaydon,[7] Schiff,[5] Gardiner,[3] and Schott[4] were not entirely consistent in their treatments of the third body M, though they were in accord for the bi-radical reaction of O and H. Gaydon *et al.*[7] presumed that a direct bi-radical reaction formed OH* in an unstable $^2\Sigma^-$ state and was followed by a radiationless transition to the stable $^2\Sigma^+$ state in order to explain the features obtained by flame spectroscopy. They posited three body collisions of O, H, and M to form OH* as the main process of OH* formation in a flame, through a consideration of the heat of formations. Schiff *et al.*[5] regarded the chemical excitation of OH* as a bi-radical reaction without a third body in their O and H association process in a low pressure flow system. Gardiner *et al.*[3] and Schott *et al.*[4] proposed a bi-radical reaction with or without a third body M to represent the OH* formation in their shock tube reaction of H_2 and O_2.

In the present study, we treated the chemical excitation process with a third body M to obtain a tentative pre-exponential factor and activation energy of the rate constant for formation of OH*. Thus, the reaction which includes OH* may be written as follows:

$$O + H + M = OH^* + M \quad (a)$$

$$OH^* + M' = OH + M' \quad (b)$$

$$OH^* = OH + h\nu \quad (c)$$

The fate of the OH* formed in reaction (a) is to follow either the non-radiative quenching process (b) in which a third body M′ is considered, or the radiative process (c) whose emission in the partial equilibrium region is now under consideration.

The reverse process (b) could be explained as a thermal excitation of OH. The activation energy of the thermal excitation process was assumed to be 93.4 kcal/mol, whereas the chemical excitation process to form OH* was characterized by a much smaller activation energy.[3] In the temperature region lower than 2000 K,[3] the contribution of the thermal excitation process to form OH* seemed to be less dominant than the chemical excitation process. The features of thermally excited OH* will be shown later in Fig. 6, along with the concentration profiles; here both chemical and thermal processes are taken into ac-

* The University of Texas at Austin, Austin, Texas, 78712 U. S. A.

count. The reverse reaction (c) is a self-absorption process whose extinction coefficient is very small.[8]

The steady state assumption of [OH*] leads to the equation:

$$[OH^*] = k_a[O][H][M]/(k_{-a}[M]+k_b[M']+k_c) \quad (1)$$

where the reverse processes (b) and (c) are disregarded by comparison with reaction (a). The reverse reaction (a) is a endothermic reaction of about 12 kcal/mol, whereas the reaction (b) is a exothermic reaction of 93.4 kcal/mol. The term $k_{-a}[M]$ is assumed to be very small compared with the term $k_b[M']$.

Bennett and Dalby[9] obtained the radiation life time of OH* and the collision cross-section between OH* and H_2O. Accepting their collision cross-section of 70 Å^2, the rate constant of reaction (b) could be evaluated by collision theory as:

$$k_b = 8.22\times10^{13}\times T^{0.5} \quad (cm^3\ mol^{-1}\ s^{-1}) \quad (B1)$$

and the value of k_c from the radiation life time is:

$$k_c = 9.9\times10^5 \quad (s^{-1}) \quad (C1)$$

In the partial equilibrium region, the concentration of H_2O computed under a sample condition of P_1=10 Torr and T_2=1500 K with $H_2/O_2/Ar$=2/2/96 is 2.5×10^{-8} mol/cm^3; then the value of $k_b[M']$ is 8.0×10^7 (s^{-1}). Thus, the value of k_c is 1/80 of the value of $k_b[M']$. If the other collision partners of OH* are taken into account along with H_2O, the value of k_c is far less than that of $k_b[M']$ and the term k_c in the denominator of Eq. 1 could reasonably be neglected. Therefore, the emission intensity I in the partial equilibrium region is given by:

$$I = Ck_c[OH^*] = Ck_ck_a[O][H][M]/k_b[M'] \quad (2)$$

where C is a correlation factor for the detector.

A sample oscillogram of an OH* emission profile is shown in Fig. 2b, along with a laser schlieren trace. In the partial equilibrium region, the OH* emission exhibits a flat plateau for the present mixtures of $H_2/O_2/Ar$=2/2/96. In Fig. 3, the OH* emission intensity I obtained from the oscillogram plateau height at various starting pressures is plotted against the concentration product of O and H of the computer simulations for each of the starting pressures. The validity of Eq. 2 and also that of reaction (a) are accordingly established by the linear relations shown in Fig. 3.

As noted previously, the computer program for the simulation requires a reaction mechanism with the forward rate constants, and the reverse rate constants incorporated into the calculation are determined from the equilibrium constants based on the JANAF thermochemical tables. The aggregation of elementary reactions and the rates used in the present work are shown in Table 1.

It is obvious that C and k_c in Eq. 2 are independent of temperature, and the activation energy of reaction (b) could be very small, as it is the rate constant for the reaction of highly activated OH*. The temperature dependence of the value of [O][H] can be evaluated from Fig. 4, where the concentration products of O and H of the computer simulations are plotted against $1/T$. The slope of the linear relations or pseudo-

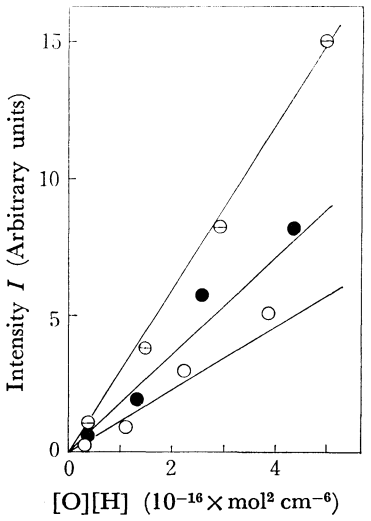

Fig. 3. The relation between emission intensity I and concentration product of [O] and [H] for different temperatures ($T\pm30$ K).
⊖: 1920 K, ●: 1550 K, ○: 1330 K.

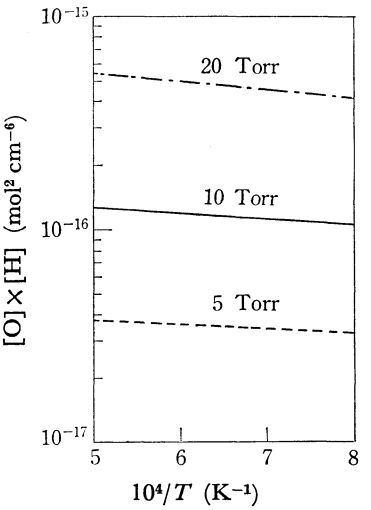

Fig. 4. The relation between concentration product ([O][H]) and $1/T$ for different starting pressures.

activation energy of the product, [O][H], is not so dominant. The above results yield the pseudo-activation energy of the product, [O][H], as 2500±700 cal/mol, where the limit of ±700 cal/mol represents the calculation's sensitivity to the variations (10-folds to 1/10-folds) of each of the rate constants in Table 1, except for the constant for the chain branching reaction of $H+O_2=OH+O$. For the latter rate constant, nearly equal values of the limit were obtained by 2-folds to 1/2-folds of the variations. The temperature dependence of the value of [M]/[M'] will be much less than that of the concentration product of O and H. Thus, it is concluded from Eq. 2 that the temperature dependence of I is the consequence of the temperature dependences of k_a and the [O][H] product in the temperature region where the thermal excitation is less dominant.[3] In Fig. 5, the emission intensity I in the partial equilibrium region was plotted against $1/T$. The apparent activation energy of the slopes

Table 1. Elementary reactions and kinetic parameters
$k=AT^n \exp(-E/RT)$ (cal, mol, cm, s units)

Reaction		A	n	E	Reference
$H_2+M=2H+M$	M=Ar, O_2	2.23×10^{12}	0.5	92600	11)
	$M=H_2$	5.58×10^{12}	0.5	92600	12)
	M=H	4.46×10^{13}	0.5	92600	12)
	$M=H_2O$	1.34×10^{13}	0.5	92600	13)
$O_2+M=2O+M$	M=Ar, H_2	1.85×10^{11}	0.5	95700	14)
	M=O	5.55×10^{12}	0.5	95700	14)
	$M=O_2$	1.85×10^{12}	0.5	95700	14)
$H_2+O_2=2OH$		2.0×10^{11}		20000	8)
$H+O_2=OH+O$		1.22×10^{17}	−0.91	16600	15)
$O+H_2=OH+H$		1.6×10^{14}		13500	16)
$OH+H_2=H_2O+H$		5.2×10^{13}		6500	16)
$H+O_2+M=HO_2+M$	$M\neq H_2O$	2.0×10^{15}		−870	17)
	$M=H_2O$	5.0×10^{16}		−870	17)
$H+OH+M=H_2O+M$	$M\neq H_2O$	7.5×10^{23}	−2.6		18)
	$M=H_2O$	1.5×10^{25}	−2.6		18)
$HO_2+H=2OH$		6.0×10^{13}			19)
$HO_2+O=OH+O_2$		1.0×10^{13}			19)
$OH+OH=H_2O+O$		5.5×10^{13}		7000	16)
$H_2+HO_2=H_2O+OH$		2.0×10^{11}		24000	20)

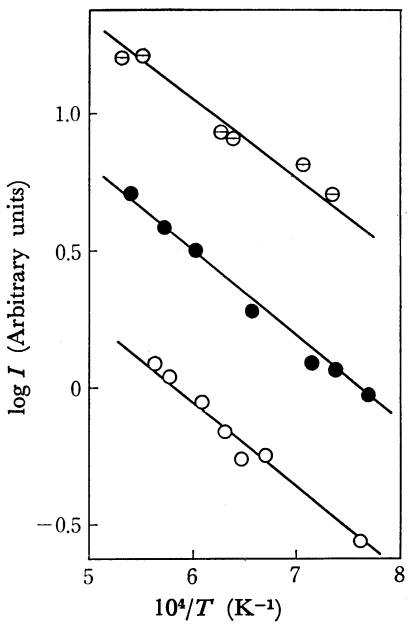

Fig. 5. The relation between log I and $1/T$ for different starting pressures.
⊖: 20 Torr, ●: 10 Torr, ○: 5 Torr.

in Fig. 5, which depends on the activation energy of k_a and the pseudo-activation energy of the [O][H] product, was obtained from the figure to be 13500 cal/mol. Thus the activation energy of k_a could be estimated from the above values as the difference, 13500—2500 cal/mol, and k_a could be expressed as:

$$k_a = A\exp(-11000\ \text{cal}/RT) \qquad (A1)$$

where A represents the pre-exponential factor of k_a. It is subjected to the following speculations.

The reaction mechanism shown in Table 1, used in the computation of the [O][H] product, does not include reactions which involve OH* because the concentration of OH* is much less than that of ordinary radicals.

To simulate the profile of OH* in the reaction, we added reactions (a), (b), and (c) to the above mechanism with the forward rate constants expressed in (A1), (B1), and (C1). Along with the rate constant expressed in (B1), we added the following rate constant (B2), evaluated by collision theory in which the collision partner is taken to be O_2 with the collision cross section of 7 Å^2, after Carrington.[10]

$$k_b = 1.84\times10^{12}\times T^{0.5}\ (\text{cm}^3\,\text{mol}^{-1}\,\text{s}^{-1}) \qquad (B2)$$

As the third body M of Eq. (a), Ar was employed in the course of the reaction simulations. For OH* and $h\nu$, the thermochemical properties were calculated by the equations based on the Mayer and Mayer representations in the JANAF thermochemical tables.[6] The mass of OH* and $h\nu$ were assumed to be OH*=OH and $h\nu=E/c^2$, where E corresponds to the 306.7 nm emission and c is the light velocity. The latter mass was provisionary assigned to carry out the computer program.

In Fig. 6, the calculated OH* concentration in the partial equilibrium region is shown *vs.* $1/T$, with parameters of the pre-exponential factor A of the expression (A1). It is obvious that the slopes of the curves depend on the parametric values of A. Calculations testing the sensitivity to reasonable variations in other rate constants showed that the pre-exponential factor has almost the total effect on the slopes of log-[OH*] *vs.* $1/T$ in a definite temperature region. As the emission intensity I is proportional to the OH* concentration in the partial equilibrium region, the slope of log I *vs.* $1/T$ should accord with that of log-[OH*] *vs.* $1/T$. The observed slope in Fig. 5 was fitted to the curve in Fig. 6, as is shown by thick line

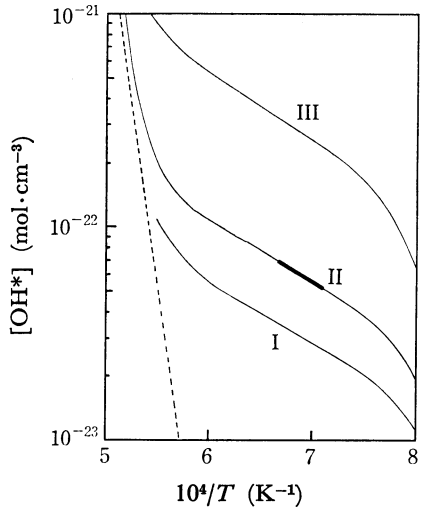

Fig. 6. The relation between calculated [OH*] and $1/T$. Broken line; The reactions (b) and (c) are taken into account. Solid line; The reactions (a), (b), and (c) are taken into account with the different A values of Eq. (A1).
I: $A=5.0\times10^8$, II: $A=1.0\times10^9$, III: $A=5.0\times10^9$.

in the latter figure. The best fit in the temperature range of 1400—1500 K was obtained when the parameter A was chosen to be 1.0×10^9 (cm^6 mol^{-2} s^{-1}).

Thus, we tentatively obtained the pre-exponential factor of reaction (a) assuming Ar as the collision partner M of the reaction. The rate constant k_a is expressed as:

$$k_a = 1.0\times10^9 \exp(-11000\ \text{cal}/RT) \quad (\text{cm}^6\ \text{mol}^{-2}\ \text{s}^{-1})$$

In the above expression of k_a, the activation energy is subjected to the error limit of the above discussion. Further investigations such as detection of the absolute emission intensity I are required to obtain a more rigorous pre-exponential factor A of the constant k_a.

The authors are grateful to Professor W. C. Gardiner, Jr. and Dr. C. B. Wakefield for providing us with the computer program "NIP", which was very helpful for the present studies.

References

1) W. E. Kaskan, *J. Chem. Phys.*, **31**, 944 (1959).
2) F. E. Belles and M. R. Lauver, *J. Chem. Phys.*, **40**, 415 (1964).
3) W. C. Gardiner, Jr., K. Morinaga, D. L. Ripley, and T. Takeyama, *Phys. Fluids Supplement*, **I**, 120 (1969).
4) D. Gutman, R. W. Lutz, N. F. Jacobs, E. A. Hardwidge, and G. L. Schott, *J. Chem. Phys.*, **48**, 5689 (1968).
5) S. Ticktin, G. Spindler, and H. I. Schiff, *Discuss. Faraday Soc.*, **44**, 218 (1967).
6) "JANAF Thermochemical Tables," Dow Chemical Company (1965).
7) A. G. Gaydon and H. G. Wolfhard, *Proc. R. Soc. Ser. A*, **208**, 63 (1951).
8) D. L. Ripley, Ph. D. thesis, University of Texas (1967).
9) R. G. Bennett and F. W. Dalby, *J. Chem. Phys.*, **40**, 1414 (1964).
10) T. Carrington, *J. Chem. Phys.*, **30**, 1087 (1959).
11) A. L. Myerson and W. S. Watt, *J. Chem. Phys.*, **49**, 425 (1968).
12) T. A. Jacobs, R. R. Giedt, and N. Cohen, *J. Chem. Phys.*, **47**, 54 (1967).
13) R. W. Getzinger and L. S. Blair, *Combust. Flame*, **13**, 271 (1969); A. Gay and N. H. Pratt, "Shock Tube Research: Proceedings of the 8th Shock Tube Symposium," Chapmann and Hall (1971), No. 39.
14) W. S. Watt and A. L. Myerson, *J. Chem., Phys.*, **51**, 1638 (1969).
15) G. L. Schott, *Combust. Flame*, **21**, 357 (1973).
16) W. C. Gardiner, Jr., W. G. Mallard, M. Mcfarland, K. Morinaga, J. H. Owen, W. T. Rawlins, T. Takeyama, and B. F. Walker, "14th Symp. Combust.," The Combustion Institute (1973), p. 61.
17) D. Gutman, E. A. Hardwidge, F. A. Dougherty, and R. W. Lutz, *J. Chem. Phys.*, **47**, 4400 (1967).
18) J. B. Homer and I. R. Hurle, *Proc. R. Soc. Ser. A*, **314**, 585 (1970).
19) W. G. Browne, D. R. White, and G. R. Smookler, "12th Symp. Combust.," The Combustion Institute (1969), p. 557.
20) V. V. Voevodsky, "7th Symp. Combust.," (1959), p. 34.